Scientific Research Publishing

Open Journal of Applied Sciences, 2025, 15(4), 798-808
https://www.scirp.org/journal/ojapps
ISSN Online: 2165-3925
ISSN Print: 2165-3917

Optimization Design of Curved Wing Box Based on BP-Multi-Objective Genetic Algorithm

Zechi Yu, Qi Wang

College of Aircraft Engineering, Nanchang Hangkong University, Nanchang, China
Email: 1963864728@qq.com

How to cite this paper: Yu, Z.C. and Wang, Q. (2025) Optimization Design of Curved Wing Box Based on BP-Multi-Objective Genetic Algorithm. *Open Journal of Applied Sciences*, **15**, 798-808.
https://doi.org/10.4236/ojapps.2025.154053

Received: March 11, 2025
Accepted: March 24, 2025
Published: March 27, 2025

Abstract

To address the conflict issues among structural mass, maximum deformation, and equivalent stress in traditional lightweight design of aircraft structures, and to improve optimization efficiency while reducing complexity, a multi-objective genetic algorithm optimization mechanism based on a BP neural network surrogate model was proposed. Additionally, to explore new internal structural layouts for wings, a curved beam rib configuration was adopted. The feasibility of this method was validated using the wing box of a specific aircraft as the research subject. Compared to the original wing box, the optimization mechanism achieved an 8.16% reduction in mass, a 0.42% decrease in structural deformation, and a 12.75% reduction in maximum equivalent stress, significantly enhancing structural performance. The established optimization mechanism can serve as a reference for the lightweight design of aircraft structures.

Keywords

Genetic Algorithm, Structural Optimization, Neural Network, Lightweight Design

1. Introduction

Since time immemorial, achieving high performance, structural lightweight, and cost-effectiveness of aircraft has been a common goal for all designers. Data indicates that for every 1% reduction in the structural weight of an aircraft, its performance improves by 3% to 5% [1]. Traditional structural optimization design often involves continuous modification, simulation analysis, and verification of the reliability of the aircraft model based on the designer's experience. This process requires engineers to perform iterative calculations repeatedly, resulting in a lengthy design cycle. However, the integration of optimization algorithms and computer

software has significantly reduced the research and development cycle. The internal structure of traditional straight-beam-rib wings is mostly designed based on the designer's experience, presenting a grid or simple arrangement, which limits the structural layout. Therefore, it is quite necessary to explore new beam-rib structural layouts.

Huang Chenglei *et al.* [2] studied the wing of a solar-powered UAV and applied the bidirectional evolutionary structural optimization method to perform topology optimization design on the wing ribs. As a result, the overall weight of the wing was reduced by 29.7%, effectively improving material utilization. Hu Jiaxin [3] proposed a hybrid optimization method for structural layout and sizing, introducing size variables into the traditional ground structure method and combining it with a neural network surrogate model and genetic algorithm for optimization. This method achieved a 13% weight reduction compared to the traditional ground structure method. Yang Yizhang *et al.* [4] proposed a structural optimization design method for UAV wings based on the particle swarm optimization algorithm. Although the wing weight was reduced by 28.26%, the maximum deformation, stress index, and failure index of the wing increased. Locatelli *et al.* [5] proposed a topology and sizing optimization framework, adopting curved beam rib structures during the optimization process. Using a rectangular wing box as an example, the results showed that the curved beam rib wing box had better weight reduction effects compared to the straight beam rib wing box, but some constraint parameters increased after optimization. The aforementioned researchers often focused on minimizing mass as the sole optimization objective in wing lightweight design. However, reducing mass often leads to an increase in deformation, equivalent stress, and other indices. Wing lightweight design requires a comprehensive consideration of strength, stiffness, and other performance indicators. In Locatelli's optimized wing box structure, the number of curved beam ribs significantly increased, and each rib had a single curvature state, which failed to fully reflect the advantages of curved structures.

In light of this, this paper proposes an optimization mechanism based on a BP neural network surrogate model combined with a multi-objective genetic algorithm. Using the straight beam rib wing box from Locatelli's paper as the test model, a curved beam rib wing box is designed for simulation analysis and optimization to identify the optimal internal structural layout. This method provides a reference for achieving lightweight design of wings.

2. Wing Structure and Finite Element Analysis

2.1. Wing Box Modeling and Material Properties

Under the condition of maintaining the material properties and working conditions of the wing box from Locatelli's literature, a straight beam rib wing box with a spanwise length of 400 mm, a chordwise length of 800 mm, upper and lower skins of 2 mm, beam rib thickness of 5 mm, and a section thickness of 20 mm is established. A frame with the same thickness as the skins is constructed around

the perimeter of the wing box. The internal structure of the model is shown in Figure 1.

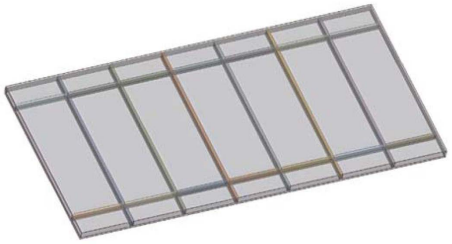

Figure 1. Wing box structural diagram.

The wing box is made of A12124-T851, a material characterized by high hardness, corrosion resistance, and significant heat treatment effects. It maintains excellent performance even under high temperatures. The material's performance parameters are listed in Table 1.

Table 1. Material properties of the wing box.

Material	A12124-T851
Young's modulus	73,100 MPa
Poisson's ratio	0.33
Density	2768 kg/m^3
Yield stress	440 MPa

2.2. Load Distribution of the Wing Box

The stress characteristics and constraints of the rectangular wing box, as described in the literature, indicate that it is subjected to a non-uniformly distributed load. The load condition is such that at the leading edge (x = 0 mm), the pressure load is 0.31 MPa, while at the trailing edge (x = 800 mm), the load is 0.142 MPa. This can be approximated as a linearly varying load distributed along the chordwise direction. A schematic diagram of the load distribution is shown in Figure 2.

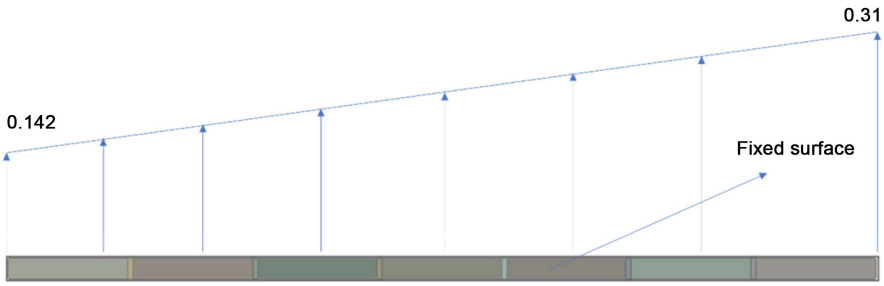

Figure 2. Load distribution of the wing box.

2.3. Simulation Analysis of the Wing Box

The constructed wing box model is imported into ANSYS software for static sim-

ulation analysis. Since the model is a three-dimensional solid model, the default solid element type, namely Solid186, is selected in the Workbench static module. This solid element type is more intuitive and capable of calculating local stress concentrations.

In finite element analysis, mesh generation is a crucial step that directly affects the accuracy of subsequent calculation results [6]. The density of the mesh and the refinement zones significantly influence the finite element calculation results. However, more and denser meshes do not necessarily lead to more accurate results. Ideally, the mesh should be selected based on the point where the calculation results no longer exhibit significant fluctuations with further refinement. The Automatic adaptive meshing method is employed, with quadrilateral elements as the unit type. The mesh is divided into sizes of 2.2 mm, 2.5 mm, 2.8 mm, 3 mm, 3.5 mm, 4 mm, 4.5 mm, 5 mm, 7 mm, and 9 mm, and the equivalent stress and deformation are calculated for each. The specific values are shown in Table 2.

Table 2. Results of wing box mesh independence verification.

Grid Size/mm	Grid quantity	Maximum stress/MPa	Maximum deformation/mm
2.2	1,041,017	111.21	3.2579
2.5	727,302	108.51	3.2574
2.8	592,097	106.74	3.2569
3	492,857	106.55	3.2567
3.5	357,137	106.001	3.2559
4	282,880	92.675	3.255
4.5	219,732	92.573	3.2536
5	172,110	89.478	3.2543
7	91,638	84.107	3.2473
9	55,611	75.24	3.2372

As shown in the table data, a mesh size of 3 mm is selected. The mesh density is 0.86 and the results of the static analysis are illustrated in Figure 3.

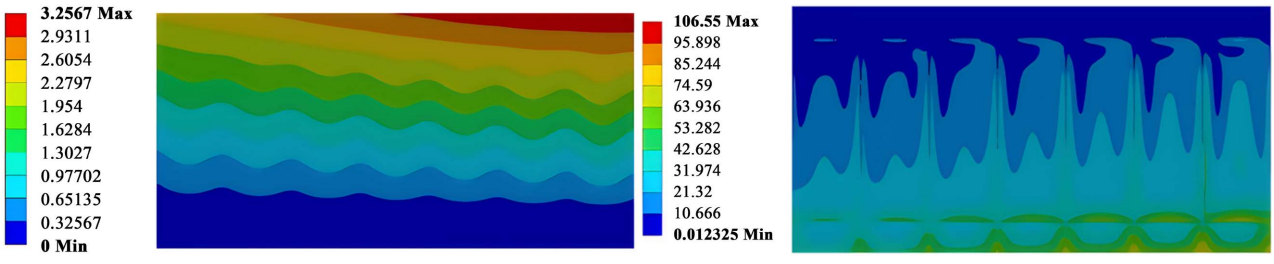

(a) (b)

Figure 3. Simulation analysis contour of the straight beam rib wing box. (a) Wing box deformation contour; (b) Wing box maximum equivalent stress contour.

As shown in Figure 3, the deformation of the wing box is smallest at the fixed surface and gradually increases along the spanwise direction, with more noticeable deformation at the corners away from the fixed end. The maximum equivalent stress of the wing box is higher at the fixed surface and gradually decreases along the spanwise direction, approaching zero at the outermost edge. Due to the wing box bearing a non-uniform distributed load, both the structural deformation and the maximum equivalent stress values increase gradually from the leading edge to the trailing edge. The mass of the wing box is 4.62 kg, the maximum deformation is 3.2567 mm, and the maximum equivalent stress is 106.55 MPa.

2.4. Simulation Analysis of the Curved Wing Box

When modeling the curved beam rib structure, it is necessary to consider how to optimize the curve in subsequent steps. A three-point control method is adopted, where the initial point, intermediate control point, and endpoint are used as curve control points. A B-spline curve is used to connect these three points, and then the wing box model is established. The mass of the curved beam rib wing box is kept the same as that of the straight beam rib wing box. The model is imported into ANSYS software for simulation analysis. The curved wing box has a mass of 4.62 kg, a maximum deformation of 3.2345 mm, and a maximum equivalent stress of 99.837 MPa. The structural diagram and simulation contour of the curved wing box are shown in Figure 4.

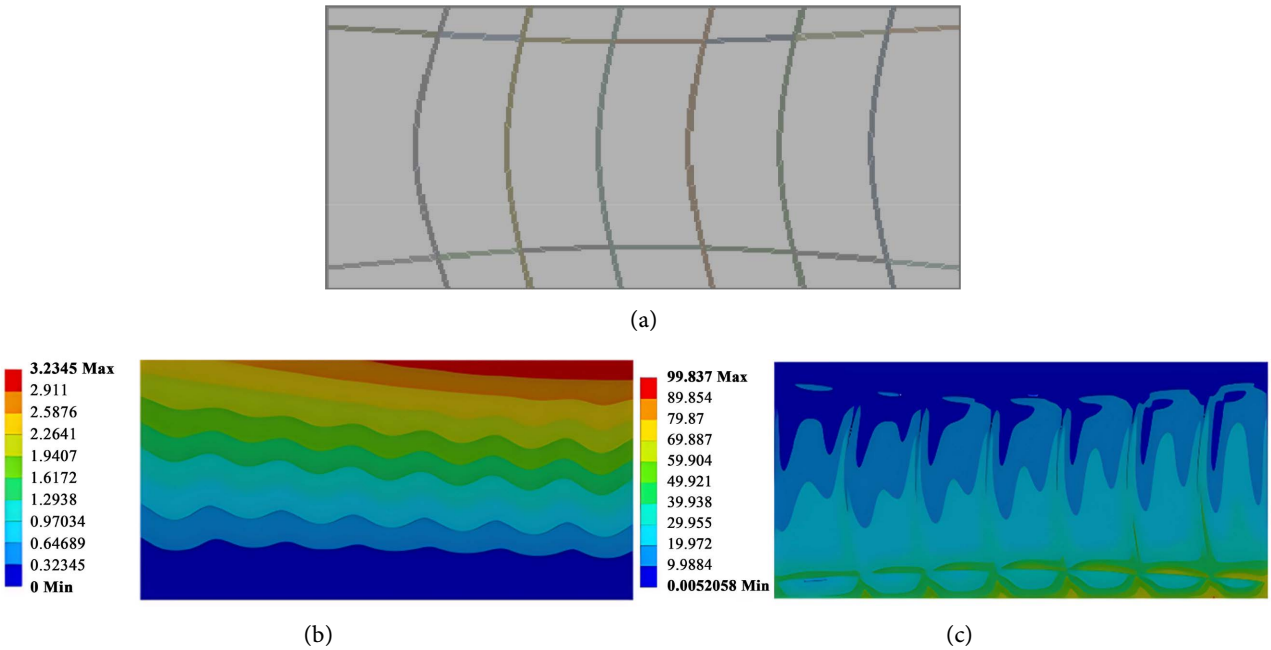

Figure 4. Simulation analysis diagram of the curved wing box. (a) Structural diagram of the curved wing box. (b) Maximum deformation contour of the curved wing box. (c) Maximum equivalent stress contour of the curved wing box.

As shown in Figure 4, under the condition of equal mass, the maximum deformation of the curved wing box is reduced by 0.68%, and the maximum equivalent

stress is reduced by 6.3%. Compared to the straight beam rib wing box, this solution demonstrates superior performance.

3. Optimization Solution

In multi-objective optimization problems, multiple objectives are often conflicting. The use of evolutionary algorithms can effectively balance the coupling between these objectives [7], making them an increasingly important tool for solving multi-objective optimization problems in many fields. However, using evolutionary algorithms to address multi-objective optimization problems requires a large number of real evaluations, which often consumes significant time, manpower, and financial resources. The use of surrogate models can accelerate the optimization process and help improve design efficiency.

This paper conducts a multi-objective structural optimization design for the curved beam rib wing box based on the BP-Multi-Objective Genetic Algorithm optimization mechanism. First, the control points of all curves in the curved wing box and the thickness values of each beam rib are taken as the design variables for structural optimization. The multi-objective optimization of the wing box structure is achieved by combining the BP neural network surrogate model and the multi-objective genetic algorithm. To ensure the surrogate model has high accuracy, the Latin Hypercube Sampling method [8] is used to sample the design variables, with 5% of the data set selected as the test set for the samples.

3.1. BP Neural Network Surrogate Model

3.1.1. Advantages of BP Neural Network

The BP neural network [9] is one of the most widely used models in artificial neural networks (ANN). It is inspired by the neurons in the biological brain and mimics the human brain's response to external stimuli, establishing a brain-like perception system. Through the forward propagation of information and the backward propagation of errors, it repeatedly learns and trains, resulting in an intelligent network. The advantages of the BP neural network are as follows:

1) Strong Approximation Capability

The BP neural network has powerful mapping and prediction abilities for solving complex problems. With reasonable sample data, a three-layer neural network structure can predict accurate solutions with high precision, making the BP neural network particularly suitable for problems with complex internal mechanisms.

2) Fault Tolerance

The BP neural network allows for minor errors during training. Even if some neurons are compromised, the overall training results are not significantly affected, demonstrating a certain level of fault tolerance.

3) Self-Learning and Adaptability

Once parameters are set, the BP neural network can autonomously conduct training and learning, storing the learned information in the network's weights. It iteratively trains until the error falls within an acceptable range.

The BP neural network is one of the foundational models of deep learning.

3.1.2. Establishment of the BP Neural Network

The BP neural network consists of an input layer, hidden layers, and an output layer. The hidden layers can be single or multiple, with each layer containing a certain number of nodes. Nodes between layers are interconnected and represented by weights. Generally, a three-layer neural network can effectively solve problems. The number of nodes in the hidden layer of the neural network can be determined using an empirical formula [10], as shown in Equation (1).

$$p = \sqrt{n + l} + \partial \tag{1}$$

here, n represents the number of input layer nodes, determined by the number of input variables, and l represents the number of output layer nodes, determined by the output variables. α is a constant between 1 and 10. In this chapter, the design variables are the parameters of all control points in the wing box and the thickness values of the beam ribs. A single hidden layer neural network is used, and the number of hidden layer nodes is automatically calculated by MATLAB based on the formula. Before training the neural network, Latin Hypercube Sampling is first performed on all design variables of the curved wing box, and the structural performance of each sample is calculated. From the sample dataset, 50 data points are selected to check the quality of the network. MATLAB calculations determine that the optimal number of hidden layer nodes is 16. The prediction regression plot, mean squared error plot, and validation point error plot are shown in Figures 5-7, respectively.

As shown in Figure 5, the neural network prediction regression R-value has high accuracy. From Figure 6, it can be seen that the mean squared error (MSE) of the BP neural network is small, meeting the program's error requirements. Figure 7 shows that the maximum stress error of randomly selected validation points ranges between 0.08% and 3.26%, with most validation point errors below 2%. The maximum deformation prediction error ranges between 0.06% and 1.24%, and the mass prediction error ranges between 0.07% and 0.28%. Combined with

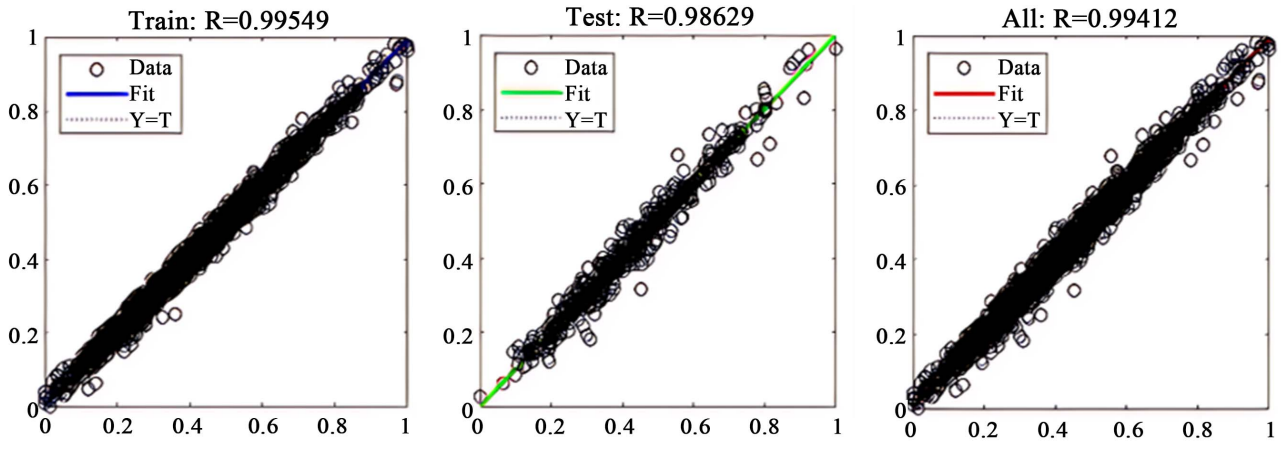

Figure 5. Prediction regression plot.

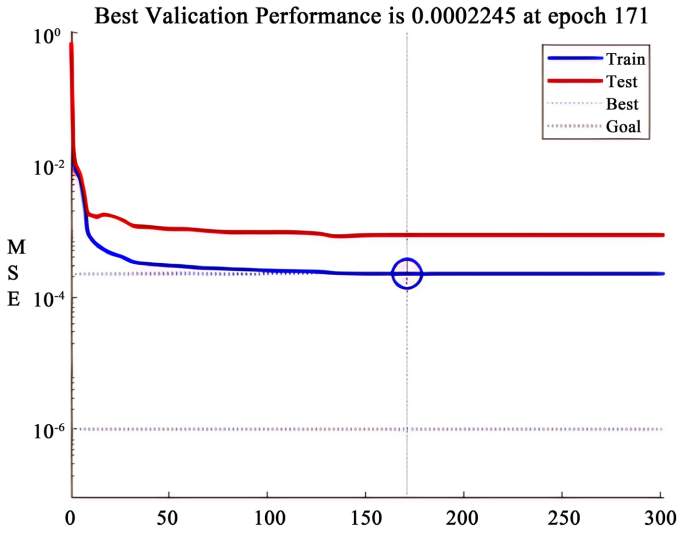

Figure 6. Mean squared error plot.

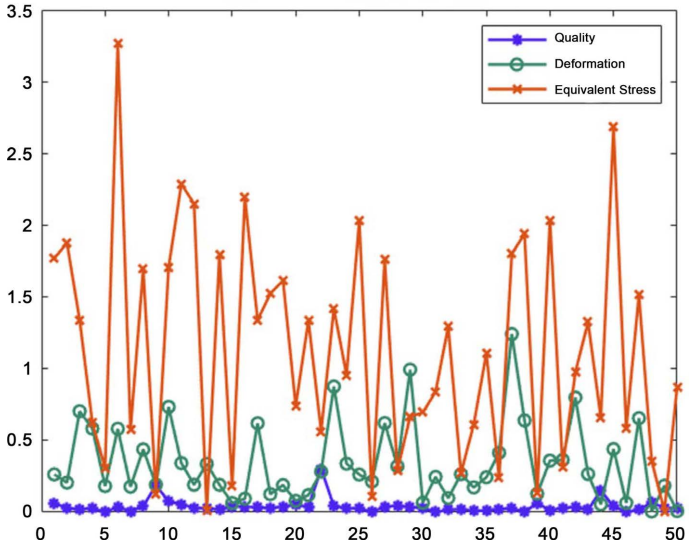

Figure 7. BP neural network prediction error percentage.

the regression R-value in Figure 5 and the prediction variance MSE in Figure 6, it indicates that the neural network has high prediction accuracy.

3.2. Multi-Objective Genetic Algorithm

The Fast Non-Dominated Sorting Genetic Algorithm with Elitist Strategy (NSGA-II) [11] is a classic multi-objective genetic algorithm. It balances multiple objectives through non-dominated sorting and crowding distance calculation. When generating offspring, non-dominated sorting is performed, where solutions with higher rankings are retained, while those with lower rankings undergo crossover and mutation. The optimal solutions computed by the NSGA-II algorithm are evenly distributed, and its convergence and robustness are superior to other multi-objective optimization algorithms [12]. It has significant advantages in the field of air-

craft structural design, as detailed below:

1) The multi-objective genetic algorithm can simultaneously optimize multiple conflicting objectives (such as structural mass, deformation, and stress) without simplifying the problem into a single-objective optimization.

2) The genetic algorithm, based on population evolution, can search for the solution space globally, avoiding getting trapped in local optima.

3) Through operations such as crossover and mutation, the diversity of solutions is increased, enhancing the probability of finding the global optimal solution.

4) The multi-objective genetic algorithm provides designers with multiple feasible optimization solutions, facilitating the trade-off between different objectives. In aircraft design, the most suitable structural design solution can be selected based on performance requirements.

The mathematical model of the multi-objective genetic algorithm in this paper is shown in Equation (2):

$$\begin{aligned} &\text{Min } F(x) = \left(f_{\text{mass}}(X), f_{\text{deformation}}(X), f_{\text{stress}}(X) \right) \\ &s.t. \begin{cases} \beta < 3.23 \text{ mm} \\ \sigma < 100.16 \text{ MPa} \\ X \in (M_i, N_i) \end{cases} \end{aligned} \tag{2}$$

here, $f_{\text{mass}}(X)$ is the mathematical model for mass, $f_{\text{deformation}}(X)$ is the mathematical model for maximum deformation, and $f_{\text{stress}}(X)$ is the mathematical model for maximum equivalent stress. B represents the maximum deformation of the structure, σ represents the maximum equivalent stress of the structure, X represents the structural design variables, and Miand Nidenote the upper and lower limits of the variables.

4. Optimization Results

This paper employs the NSGA-II algorithm to optimize the BP neural network model established in Chapter 2.1. Three candidate points with the minimum mass, minimum deformation, and minimum maximum equivalent stress are selected from the solution set, as shown in Table 3 below.

Table 3. Comparison of wing box data.

	Mass/kg	Deformation/mm	Equivalent Stress/MPa
Candidate Point 1	4.2481	3.2312	91.417
Candidate Point 2	4.6196	3.0678	84.0036
Candidate Point 3	4.5870	3.1797	75.7779

As shown in Table 3, Candidate Point 1 has the minimum mass, and both the deformation and equivalent stress of the wing box are reduced. Although Candidate Points 2 and 3 show significant reductions in deformation and stress, their

masses are not significantly different from the original structure. Finally, simulation analysis is performed on all candidate points, and the design parameters of the candidate point with the minimum mass are selected for re-simulation analysis of the wing box. The results are shown in Figure 8.

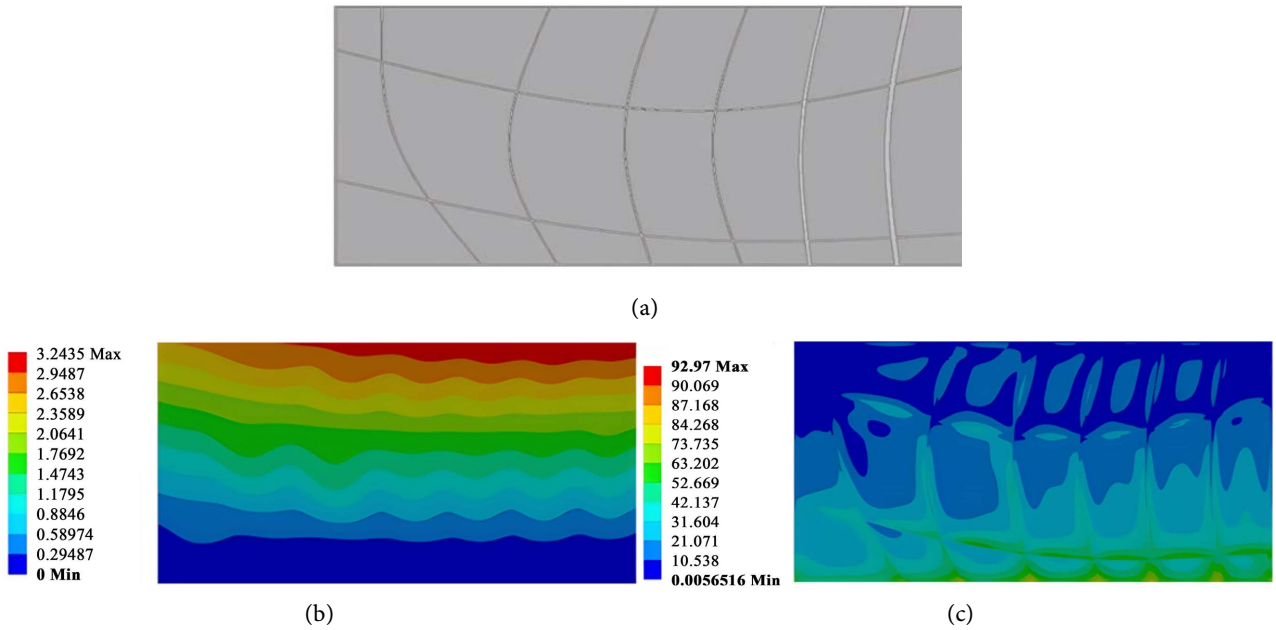

(a) (b) (c)

Figure 8. Simulation contour of the curved wing box. (a) Structural diagram of the curved wing box. (b) Deformation contour of the curved wing box. (c) Maximum equivalent stress contour of the curved wing box.

As shown in Figure 8, the internal structure of the wing box features different curve layouts and thicknesses for each beam rib. While the maximum deformation remains largely unchanged, the equivalent stress is significantly reduced and is mostly concentrated at the fixed surface, with stress distribution being more uniform elsewhere. Compared to the original wing box, the optimized wing box achieves an 8.16% reduction in mass, a 0.41% reduction in maximum deformation, and a 12.75% reduction in maximum equivalent stress. This demonstrates that the multi-objective optimization method effectively reduces the mass, deformation, and equivalent stress of the wing box, enhancing its structural performance while achieving lightweight design.

5. Conclusions

For the optimization design of the curved structure of the wing box, this study adopts a BP-Multi-Objective Genetic Algorithm optimization mechanism. The main conclusions are as follows:

1) By applying the BP-Multi-Objective Genetic Algorithm to optimize the curved wing box, compared to single-objective optimization, this method comprehensively considers the coupling relationships among multiple objectives. The optimized results show an 8.16% reduction in mass, a 0.41% reduction in maximum deformation, and a 12.75% reduction in maximum equivalent stress, demonstrat-

ing excellent optimization performance.

2) After optimization of the curved beam rib wing box, the curved structure of each beam rib varies. Compared to the original wing box structure, the curved structure exhibits superior performance.

There are still some limitations in the study of the curved wing box in this paper. Future research could consider lightweight design for other aircraft structures, or even conduct lightweight design for the entire wing structure combined with fluid-structure interaction analysis.

Conflicts of Interest

The authors declare no conflicts of interest regarding the publication of this paper.

References

[1] Xie, X.H. (2020) Research on Lightweight Design of the Main Load-Bearing Structure of a Large Aircraft Landing Gear. Master's Thesis, Nanjing University of Aeronautics and Astronautics.

[2] Huang, C.L., Fan, Q.M., Liu, H.J., *et al.* (2024) Topology Optimization Design of Wing Rib Based on Bi-Directional Evolutionary Structural Optimization Method. *Journal of Northwestern Polytechnical University*, **42**, 1005-1010. https://doi.org/10.1051/jnwpu/20244261005

[3] Hu, J.X., Rui, S., Gao, R.C., *et al.* (2022) A Hybrid Optimization Method for Aircraft Structural Layout and Sizing. *Acta Aeronautica et Astronautica Sinica*, **43**, 368-378.

[4] Yang, Y.Z. and Liao, Y.Q. (2023) Structural Optimization Design of UAV Wing Based on Particle Swarm Algorithm. *Internal Combustion Engine and Parts*, No. 6, 93-96.

[5] Locatelli, D. (2012) Optimization of Supersonic Aircraft Wing-Box Ueing Curvilinear Sparib-s. Virginia Tech.

[6] (2013) ANSYS Workbench Advanced Applications in Structural Engineering. China Water & Power Press.

[7] Sun, Z.R., Huang, Y.H. and Chen, Z.Y. (2021) A Diversity-Based Surrogate-Assisted Evolutionary Algorithm for Multi-Objective Optimization. *Journal of Software*, **32**, 3814-3828.

[8] He, X.Y., Zhang, J., Qin, T., *et al.* (2024) An Improved Coot Algorithm Based on Latin Hypercube Sampling. *Computer Engineering and Design*, **45**, 1069-1078.

[9] Li, M.H. (2016) Application of Artificial Neural Networks Combined with Intelligent Algorithms in Structural Optimization. Master's Thesis, Guangzhou University.

[10] Qiu, D.P. (2024) Research and Case Study on the Hidden Layer Structure of BP Neural Networks. *Changjiang Information and Communication*, **37**, 8-10.

[11] Xing, B.F. and Xu, W. (2023) Load Path Analysis and Multi-Objective Genetic Algorithm Optimization of UAV Wing Beam Joints. *Science Technology and Engineering*, **23**, 10127-10132.

[12] Yan, J.W., Lu, Z.D. and Zhou, X. (2021) Multi-Objective Optimization of Equipment Operation Parameters in Cold Source Equipment Rooms Based on NSGA-II. *Science Technology and Engineering*, **21**, 2896-2903.